British Journal of Pharmacology (1996) 118, 748–754

Endogenous calcium channels in human embryonic kidney (HEK293) cells

Stanislav Berjukow, Frank Döring, Monika Froschmayr, Manfred Grabner, Hartmut Glossmann & [1]Steffen Hering

Institut für Biochemische Pharmakologie, Universität Innsbruck, A 6020 Innsbruck, Austria

1 We have identified endogenous calcium channel currents in HEK293 cells. Whole cell endogenous currents ($I_{Sr\text{-}HEK}$) were studied in single HEK293 cells with 10 mM strontium as the charge carrier by the patch clamp technique. The kinetic properties and pharmacological features of $I_{Sr\text{-}HEK}$ were characterized and compared with the properties of a heterologously expressed chimeric L-type calcium channel construct.

2 $I_{Sr\text{-}HEK}$ activated on depolarization to voltages positive of −40 mV. It had transient current kinetics with a time to peak of 16±1.4 ms ($n=7$) and an inactivation times constant of 52±5 ms ($n=7$) at a test potential of 0 mV. The voltage for half maximal activation was −19.0±1.5 mV ($n=7$) and the voltage for half maximal steady-state inactivation was −39.7±2.3 mV ($n=7$).

3 Block of $I_{Sr\text{-}HEK}$ by the dihydropyridine isradipine was not stereoselective; 1 μM (+) and (−)-isradipine inhibited the current by 30±4% ($n=3$) and 29±2% ($n=4$) respectively. (+)-Isradipine and (−)-isradipine (10 μM) inhibited $I_{Sr\text{-}HEK}$ by 89±4% ($n=5$) and 88±8% ($n=3$) respectively. The 7-bromo substituted (±)-isradipine (VO2605, 10 μM) which is almost inactive on L-type calcium channels also inhibited $I_{Sr\text{-}HEK}$ (83±9%, $n=3$) as was observed for 10 μM (−)-nimodipine (78±6%, $n=5$). Interestingly, 10 μM (±)-Bay K 8644 ($n=5$) had no effect on the current. $I_{Sr\text{-}HEK}$ was only slightly inhibited by the cone snail toxins ω-CTx GVIA (1 μM, inhibition by 17±3%, $n=4$) and ω-CTx MVIIC (1 μM, inhibition by 20±3%, $n=4$). The funnel web spider toxin ω-Aga IVA (200 nM) inhibited $I_{Sr\text{-}HEK}$ by 19±2%, $n=4$).

4 In cells expressing $I_{Sr\text{-}HEK}$, maximum inward current densities of 0.24±0.03 pA/pF and 0.39±0.7 pA/pF (at a test potential of −10 mV) were estimated in two different batches of HEK293 cells. The current density increased to 0.88±0.18 pA/pF or 1.11±0.2 pA/pF respectively, if the cells were cultured for 4 days in serum-free medium.

5 Co-expression of a chimeric L-type calcium channel construct revealed that $I_{Sr\text{-}HEK}$ and L-type calcium channel currents could be distinguished by their different voltage-dependencies and current kinetics. The current density after heterologous expression of the L-type α_1 subunit chimera was estimated to be about ten times higher in serum containing medium (2.14±0.45 pA/pF) than that of $I_{Sr\text{-}HEK}$ under the same conditions.

Keywords: Ca^{2+} channels; HEK293 cells; expression system; class E calcium channels; T-type calcium channels; 1,4-dihydropyridines

Introduction

The human embryonic kidney cell line HEK293 serves as an efficient test system for functional and biochemical studies of ionic channel proteins. This cell line can be used as a transient or stable heterologous expression system and recently became widely used for expression of voltage-dependent calcium channels (Williams *et al.*, 1994; de Leon *et al.*, 1995; Bangalore *et al.*, 1995; Kamp *et al.*, 1995; Schreieck *et al.*, 1995; Perez-Garcia *et al.*, 1995).

Many of the mammalian cell lines that are currently used for expression of voltage-dependent calcium channels, as well as *Xenopus laevis* oocytes, have been shown to express endogenous calcium channels (Adams & Beam 1989; Bourinet *et al.*, 1992; Skryma *et al.*, 1994; Lacerda *et al.*, 1994). However, it is still uncertain whether HEK293 cells express endogenous calcium channels. Precise knowledge about the current density, voltage-dependence, kinetic properties and pharmacological features of endogenous currents is a necessary precondition for studies of calcium channel α_1 subunits or subunit compositions expressed in these cells.

In the present study we demonstrated that the cell line HEK293 does express endogenous calcium channels. We describe their basic properties and suggest, that endogenous calcium channels in HEK293 cells have some kinetic and pharmacological similarities with class E or T-type calcium channels (Soong *et al.*, 1993). The endogenous calcium channels in HEK293 cells cannot, however, be attributed to a particular class of calcium channels (Birnbaumer *et al.*, 1994) because the currents are inhibited by 1,4-dihydropyridine compounds with a profile that suggest an unusual non-specific interaction in comparison to L-type calcium channels. We demonstrate that the density of endogenous calcium channel currents in HEK293 cells is increased if the cells are grown in serum-free culture medium.

By transfecting HEK293 cells with cDNA of a chimeric L-type calcium channel α_1 subunit, we illustrate that the currents of endogenous and heterologously expressed L-type calcium channels can be separated by their voltage-dependence as well as by pharmacological and kinetic properties.

Methods

Cell culture and transfection

HEK293 cells were grown at 37°C in Dulbecco's modified Eagles medium (GIBCO, Grand Island, NY, U.S.A.) containing 10% foetal bovine serum (FBS, Sebak, Suben, Austria) at 8% CO_2. For differentiation HEK293 cells were cultured in

[1]Author for correspondence at: Institut für Biochemische Pharmakologie, A-6020 Innsbruck, Peter Mayr Straße 1, Austria.

serum free (FBS-free) Optimem Medium (GIBCO) at 40–50% confluency for 4 days. Two different batches of HEK293 cells were used in the present study. Experiments with the first batch (No. F-10626) of HEK293 cells were performed between passage numbers P34 to P42. The second batch of HEK293 cells (No. F-11987) was studied between passage numbers P32 to P39.

HEK293 cells were transfected with a chimera between rabbit heart $\alpha_{1C\text{-}a}$ (H) (Mikami *et al.*, 1989) and carp skeletal muscle α_{1S} (s) (Grabner *et al.*, 1991) sH (amino acid numbers in parentheses): s(1-60), H(145-2171). As described previously substitution of the amino terminus of the $\alpha_{1C\text{-}a}$ subunit by a sequence of the carp skeletal muscle α_1 subunit resulted in a significantly higher expression rate of the resulting chimera without affecting current kinetics (Wang *et al.*, 1995). Heterologous expression experiments were routinely done with co-transfection of the β_{1a} calcium channel subunit (Ruth *et al.*, 1989).

Calcium channel subunit cDNAs were inserted into the mammalian expression vector pcDNA3 (Invitrogen) and therefore expressed under the control of a CMV promoter. HEK293 transfections were mediated by Lipofectamin (GIBCO) following the manufacturer's instructions. A standard transfection (in 35 mm Petri dishes) was done with 1 μg of each expression plasmid, 9 μl Lipofectamin at a cell density of about 70% confluency. Patch clamp experiments were performed between 36 to 48 h after transfection.

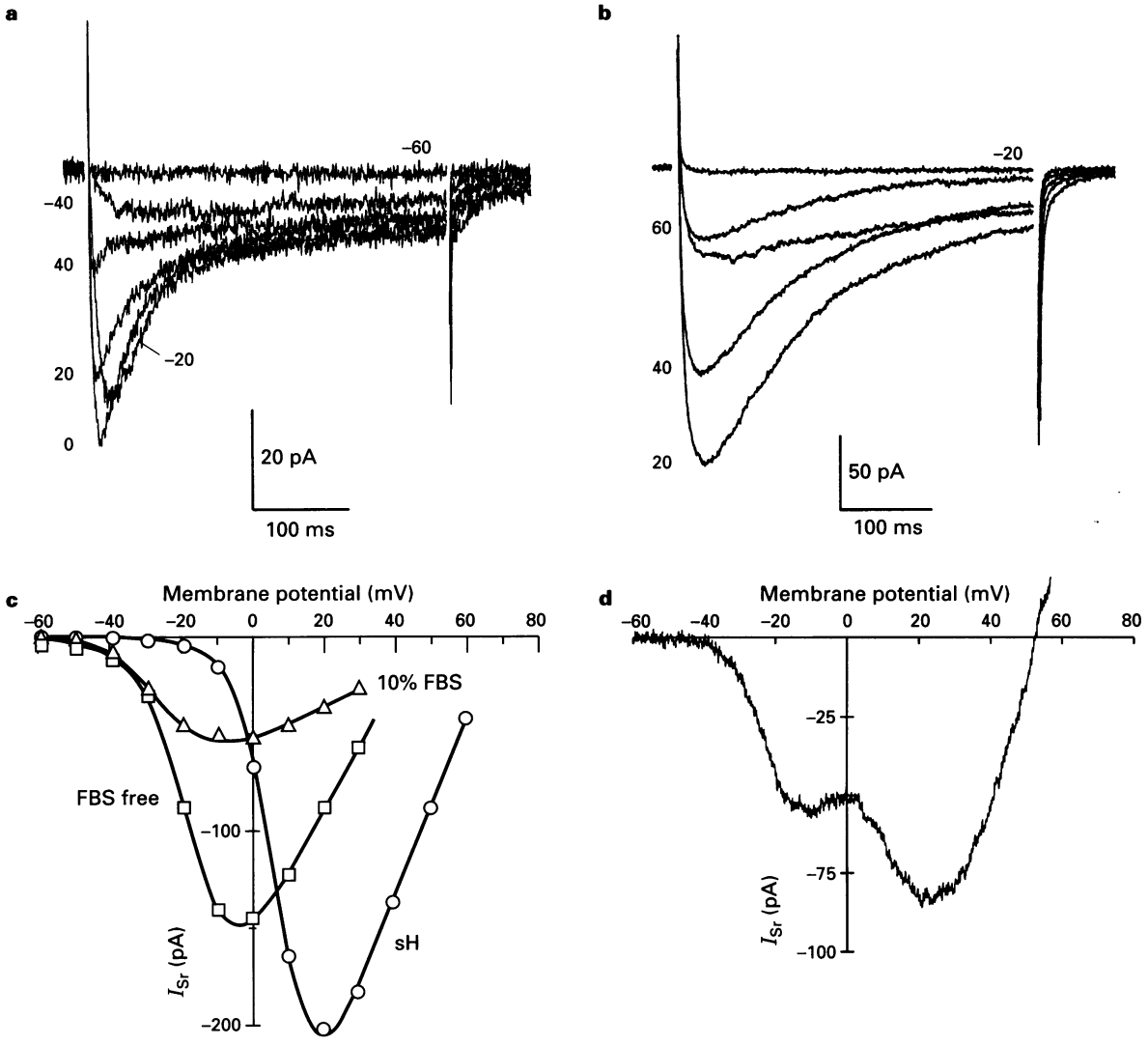

Figure 1 Strontium inward currents and current voltage relationship of $I_{Sr\text{-}HEK}$ and $I_{Sr\text{-}sH}$ in HEK293 cells: (a, b) Families of $I_{Sr\text{-}HEK}$ (cultured with 10% FBS) and $I_{Sr\text{-}sH}$ in HEK293 cells. (a) Inward currents ($I_{Sr\text{-}HEK}$) of a HEK293 cell grown for 4 days in DMEM supplemented with 10% FBS at voltages from −60 mV to 40 mV, in 20 mV voltage steps, holding potential −70 mV. (b) Inward currents ($I_{Sr\text{-}sH}$) of a HEK293 cell (cultured in DMEM supplemented with 10% FBS) which was transfected with cDNA encoding for the α_1 chimera sH (see Methods) at voltages from −20 mV to 60 mV, in 20 mV voltage steps, holding potential −50 mV (for partial inactivation of $I_{Sr\text{-}HEK}$, see Figure 2). Test potentials are indicated. (c) Peak-current-voltage relationships of calcium channel currents in HEK293 cells for $I_{Sr\text{-}HEK}$ (same experiment as shown in a), $I_{Sr\text{-}HEK}$ (cell was cultured in FBS-free medium) and $I_{Sr\text{-}sH}$ (same experiment as shown in b). Smooth lines represent the best-fit curves to the function $I_{Sr\text{-}HEK/sH} = G_{max}*(V\text{-}V_{rev})/(1+\exp[(V\text{-}V_{0.5,\ act})/k_{act}]$. $I_{Sr\text{-}HEK/sH}$, values of the peak $I_{Sr\text{-}sH}$ or $I_{Sr\text{-}HEK}$ of typical cells at a given test potential V; G_{max}, maximal conductance value; V_{rev}, reversal potential; $V_{0.5,act}$, voltage of half-maximal current activation; k_{act}, slope factor. The estimated values for k_{act} and $V_{0.5,act}$ are: $I_{Sr\text{-}HEK\ (10\%\ FBS)}$ (△) ($k_{act} = -7.53$ mV, $V_{0.5,\ act} = -24.5$ mV, $V_{rev} = 62$ mV, $G_{max} = 0.84$ pS); $I_{Sr\text{-}HEK\ (FBS\text{-}free)}$ (□) ($k_{act} = -6.7$ mV, $V_{0.5,\ act} = -16.9$ mV, $V_{rev} = 46.5$ mV, $G_{max} = 3.37$ pS); $I_{Sr\text{-}sH}$ (○)($k = -5.84$ mV, $V_{0.5,\ act} = 8.02$ mV, $V_{rev} = 68$ mV, $G_{max} = 4.73$ pS). The estimated current densities were 0.28 pA/pF (△), 0.99 pA/pF (□) and 1.5 pA/pF (○). (d) Current-voltage relationship obtained by a 300 ms ramp depolarization from −70 mV to 80 mV in a HEK293 cell 36 h after transfection with cDNA encoding for chimera sH. Note that the two peaks of the inward current correspond to the peak values of the curves obtained in (c). This protocol enables the observation of the expression of $I_{Sr\text{-}HEK}$ and $I_{Sr\text{-}sH}$ in the same cell.

Ionic current recordings and data acquisition

Inward strontium-currents were recorded in HEK293 cells at 22–25°C by the whole cell configuration of the patch-clamp technique (Hamill *et al.*, 1981) with a patch clamp amplifier (EPC 7, List electronic, Germany). Patch pipettes with resistance of 1 to 4 Mohm were made from borosilicate glass (Clark Electromedical Instruments, UK GC150-7.5) and filled with pipette solution containing (in mM): CsCl 60, CsOH 60, aspartate 60, $MgCl_2$ 2, HEPES 10, EGTA 10 titrated to pH 7.25 with CsOH. I_{Sr} were measured in external strontium solution containing (in mM): $SrCl_2$ 10, N-methyl-D-glucamine 190, HEPES 10, glucose 20, 4-aminopyridine 4, tetraethylammonium chloride 27, $MgCl_2$ 3, buffered to pH 7.3 with methanesulphonic acid.

Data were digitized using a DIGIDATA 1200 interface (Axon Instruments, Foster City, U.S.A.) and stored on the computer hard disc. Data were filtered at 1 kHz (four-pole Bessel filter) and digitized at a sampling rate of 5 kHz. Leak currents were subtracted digitally (using average values of scaled leakage currents elicited by a 10 mV hyperpolarizing pulse) or electronically by means of an analogue circuit.

Exchange of the bath solution (i.e. extracellular drug application) was achieved by means of a microperfusion chamber (MPC 50, List Electronic, Germany) enabling repeated fast solution exchange in single cells without contamination of the entire bath (see Savchenko *et al.*, 1995 for details). This technique was highly suitable for application of small amounts of the peptide toxins as 50 µl test solution were sufficient for a 20 fold exchange of the chamber volume. Before drug application cells were monitored for run-down during a period of 10 min. Only cells with a run down of less than 5% were used to study toxin or drug effects. Data are given as ranges or means ± s.e.mean. Statistical significance was calculated according to Student's unpaired *t* test for two populations.

Materials

Human embryonic kidney (HEK293) cells were obtained from the American Type Culture Collection (Rockville, MD, U.S.A.). The 1,4-dihydropyridines (+)- and (−)-isradipine and VO 2605 (isopropyl 4-(2,3,1 (7-bromo) benzoxadiazol-4-yl)-1,4-dihydro-2,6-dimethyl-5-methoxycarbonylpyridine 3-car-boxylate) were kindly provided by Sandoz AG (Basle, Switzerland) and (±)-Bay K 8644 and (−)-nimodipine were from Bayer AG (Wuppertal, Germany). ω-Agatoxin IVA (Funnel Web Spider toxin, ω-Aga IVA) was obtained from BIO TREND (Germany) and ω-conotoxin GVIA (marine snail toxin, ω-CTx GVIA) was from Peninsula Laboratories (U.S.A.). ω-Conotoxin MVIIC was from Saxon Biochemicals (Germany).

Results

Endogenous calcium channel currents were observed in 160 (76%) out of 210 non-transfected HEK293 cells with 10 mM strontium as the charge carrier. Depolarizing the cell membrane from a holding potential of −70 mV above a threshold of −40 mV evoked transient voltage-dependent inward currents.

Figure 1a shows a family of whole cell $I_{Sr\text{-}HEK}$ from a nontransfected HEK293 cell. The currents reached maximal

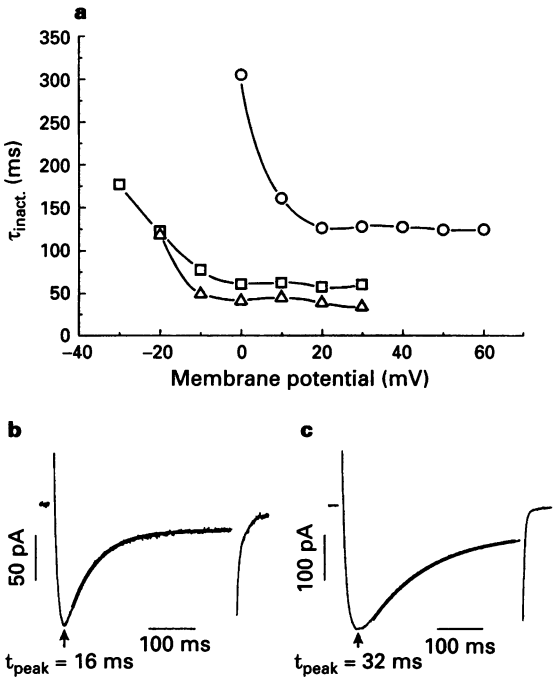

Figure 2 Comparison of activation and inactivation kinetics of $I_{Sr\text{-}HEK}$ and $I_{Sr\text{-}sH}$ in HEK293 cells. (a) Inactivation time constants of $I_{Sr\text{-}HEK}$ in non transfected and $I_{Sr\text{-}sH}$ in transfected HEK293 cells are plotted as a function of the membrane potential. $I_{Sr\text{-}HEK}$ were elicited by 400 ms depolarizing voltage steps from −70 mV to the indicated membrane potentials ($I_{Sr\text{-}HEK}$, (△) cells cultured in 10% FBS and $I_{Sr\text{-}HEK}$, (□) recorded after culturing the cells for 4 days in FBS-free medium). Alternatively $I_{Sr\text{-}sH}$ (○) were recorded during 400 ms depolarizations from −50 mV. The inactivation time course was fitted by a single exponential function. Data from three representative cells. (b,c) Solid lines represent best fit to the function $I_{Sr\text{-}HEK/sH}(t) = A^*\exp(-t/\tau_{inact}) + C$. For $I_{Sr\text{-}HEK}$ (b) $\tau_{inact} = 60$ ms (at 0 mV) and for $I_{Sr\text{-}sH}$ (c) $\tau_{inact} = 132$ ms (at 20 mV) were estimated.

Table 1 Properties of $I_{Sr\text{-}HEK}$ and $I_{Sr\text{-}sH}$ in HEK293 cells

Current type	*Current density* (pA/pF)	$V_{0.5,act}$ (mV)	k_{act} (mV)	$V_{0.5,inact}$ (mV)	$k_{inact.}$ (mV)	G_{max} (pS)	t_{peak} (ms)	τ_{inact} (ms)
$I_{Sr\text{-}HEK}$* (10% FBS)	0.24 ± 0.03**	−19.0 ± 1.5	5.7 ± 0.35	−39.7 ± 2.3	−3.6 ± 0.3	0.82 ± 0.12	16.8 ± 1.4	52 ± 5
$I_{Sr\text{-}HEK}$* (FBS-free)	0.88 ± 0.18**	−18.5 ± 1.7	5.6 ± 0.1	−41.2 ± 1.5	−3.7 ± 0.27	3.1 ± 0.2	17.0 ± 1.2	57 ± 5
$I_{Sr\text{-}sH}$* (10% FBS)	2.14 ± 0.45**	9.2 ± 1.1	5.2 ± 0.8	−10.1 ± 1.3	−5.7 ± 0.36	4.85 ± 0.93	34.0 ± 1.1	209 ± 20

Current kinetics of $I_{Sr\text{-}HEK}$ and $I_{Sr\text{-}sH}$ were studied at test potentials of 0 mV and 20 mV respectively. For $I_{Sr\text{-}HEK}$ measurements the holding potential was −70 mV. To minimize contamination of $I_{Sr\text{-}sH}$ by $I_{Sr\text{-}HEK}$ transfected cells were held at −50 mV if current kinetics of $I_{Sr\text{-}sH}$ were studied. Abbreviations: $k_{act/inact}$ slope factor of corresponding steady-state activation or inactivation curves; $V_{0.5,act/inact}$ potentials of half-maximal current activation and inactivation; τ_{inact}, inactivation time constant, t_{peak}, time to peak of the inward current. Values are the mean ± s.e.mean from 5 to 7 HEK293 cells. *Cells from batch No.F-10626, passage numbers P34 to P42. **The observed differences in current densities were highly significant: $I_{Sr\text{-}HEK}$ (10% FBS) versus $I_{Sr\text{-}HEK}$ (FBS free) $P < 0.01$.

values at -6 ± 1.0 mV ($n=7$) and reversed at 55 ± 6.1 mV ($n=7$). Voltages for half maximal activation were estimated as described in Figure 1c (see Table 1). $I_{Sr\text{-}HEK}$ recorded by voltage ramp protocols in nontransfected HEK293 cells had a single peak with no evidence for more than one calcium channel type expressed and a similar current-voltage relationship to that observed in Figure 1c (data not shown).

The time course of current inactivation during a 400 ms test depolarization was approximated by a single exponential function (Figure 2b). The calculated inactivation time constant was voltage-dependent, declining in the cell shown in Figure 2b from 117 ms at -20 mV to 34 ms at 30 mV (Figure 2a). $I_{Sr\text{-}HEK}$ activated rapidly reaching a time to peak between 14.8 ms and 18.8 ms at 0 mV (Figure 2b, see Table 1 for mean values of time to peak at a test potential of 0 mV). The voltage-dependence of calcium channel availability was determined by measuring the peak $I_{Sr\text{-}HEK}$ during a test pulse to 0 mV after a 10 s conditioning prepulse (see Figure 3). The voltage for half maximal inactivation of $I_{Sr\text{-}HEK}$ is indicated in Table 1.

Reduction or complete removal of growth factors from the culture medium induces in many cell lines a morphological differentiation and accumulation of specific gene products like calcium channel proteins (see Biel *et al.*, 1991). We have grown HEK293 cells for 4 days in FBS-free culture medium and observed a significant increase in $I_{Sr\text{-}HEK}$-density whereas the voltage-dependence and kinetics of calcium channel currents remained unchanged (Figure 1c, see Table 1 for data from cell batch No. F-10626). In a second batch of HEK293 cells (see Methods) the current density increased from 0.39 ± 0.7 pA/pF ($n=26$) to 1.11 ± 0.2 pA/pF ($n=15$) after removal of FBS from the culture medium. In previous studies L-type α_1 subunits have been expressed in the HEK293 cells but no endogenous calcium channel currents have been reported (i.e. Perez-Garcia 1993; Schreieck *et al.*, 1995). We have considered the possibility that endogenous calcium channels may appear only in certain cell batches and therefore performed experiments on two different batches of HEK293 cells with different passage numbers (see Methods). Voltage-dependence and current kinetics of $I_{Sr\text{-}HEK}$ were found to be similar in both HEK293 batches tested.

To compare voltage-dependence and kinetic properties of $I_{Sr\text{-}HEK}$ with L-type calcium channels we transfected HEK293 cells with cDNA encoding for the chimeric α_1 subunit sH (see also Wang *et al.*, 1995; Grabner *et al.*, 1996; for kinetic and pharmacological properties of construct sH). Figure 1b shows $I_{Sr\text{-}sH}$ of a HEK293 cell recorded 48 h after transfection with the corresponding cDNA. $I_{Sr\text{-}sH}$ activated and inactivated with slower current kinetics compared to $I_{Sr\text{-}HEK}$ (Figure 1a). $I_{Sr\text{-}sH}$ activated during depolarizing steps from -50 mV above a threshold of -20 mV and reached maximal current values at 20 ± 2 mV ($n=7$). The current voltage relationship of $I_{Sr\text{-}sH}$ is shown in Figure 1c (same cell as in Figure 1b, superimposed with the $I_{Sr\text{-}HEK}$ current voltage relationships of nontransfected HEK293 cells). The fact that two channel types ($I_{Sr\text{-}HEK}$ and $I_{Sr\text{-}sH}$) with different voltage-dependence are expressed in a single HEK293 cells was also evidence from the current-voltage relationship. When ramp depolarizations were applied from a holding potential of -70 mV to $+80$ mV (see Figure 1d) two peaks were distinguishable. Similar observations were made in 26 (71%) out of 37 cells expressing the L-type chimera sH. The first peak on the current-voltage relationship (Figure 1d, related to activation of $I_{Sr\text{-}HEK}$) could be reduced by holding the cells at more depolarized potentials (data not shown). At later stages after transfection (>48 h) a separate peak of $I_{Sr\text{-}HEK}$ on the current-voltage relationship was less prominent and presumably superimposed by threshold $I_{Sr\text{-}sH}$ because this channel type was expressed at a much higher density (see Table 1).

The voltage-dependence of steady state inactivation and kinetic properties of $I_{Sr\text{-}sH}$ and $I_{Sr\text{-}HEK}$ are shown in Figure 3. Compared to $I_{Sr\text{-}HEK}$, the voltage for half maximal inactivation of $I_{Sr\text{-}sH}$ was found to be about 30 mV more positive (Table 1, see also Figure 1a, b, c for the different thresholds of $I_{Sr\text{-}sH}$ and $I_{Sr\text{-}HEK}$ activation). Inactivation kinetics of $I_{Sr\text{-}sH}$ were described by a voltage-dependent time constant decaying from 276 ms at -20 mV to about 45 ms at 40 mV (Figure 2a, c; see Table 1 for mean values, of time to peak and inactivation time constants at 20 mV test potential).

The maximal current density of $I_{Sr\text{-}sH}$ in transfected cells was estimated from the peak current values obtained upon depo-

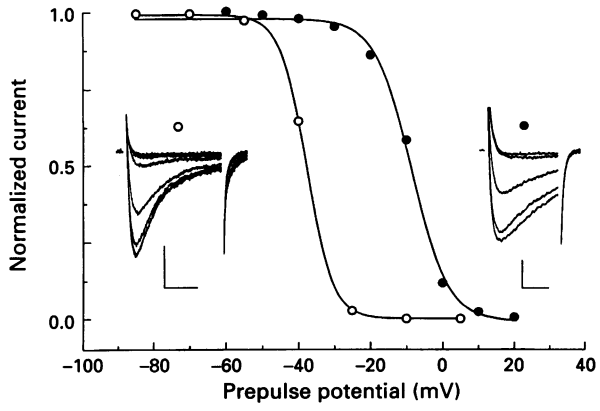

Figure 3 Steady state inactivation curves of $I_{Sr\text{-}HEK}$ and $I_{Sr\text{-}sH}$: the peak currents during a 300 ms test pulse to 0 mV ($I_{Sr\text{-}HEK}$, ○) or 20 mV ($I_{Sr\text{-}sH}$, ●) were plotted versus the voltage of a 10 s conditioning prepulse. Interpulse interval was 2 ms. Solid lines are drawn according to the equation: $I_{Sr\text{-}HEK}/I_{Sr\text{-}HEK,max} = 1/(1+\exp[(V-V_{0.5,\,inact})/k_{inact}])$; $I_{Sr\text{-}HEK}$: $V_{0.5,\,inact} = -37.5$ mV; $k_{inact} = -3.67$ mV; $I_{Sr\text{-}sH}$: $V_{0.5,inact} = -12.5$ mV, $k_{inact} = -5.95$ mV. Inset: $I_{Sr\text{-}HEK}$, (○) recorded after conditioning prepulses to -85, -70, -55, -40, -25, -10 and 5 mV, calibration bars 50 pA and 100 ms. $I_{Sr\text{-}sH}$, (●) recorded after condition prepulses to -60, -50, -40, -30, -20, -10, 0, 10 and 20 mV, calibration bars 50 pA, 100 ms.

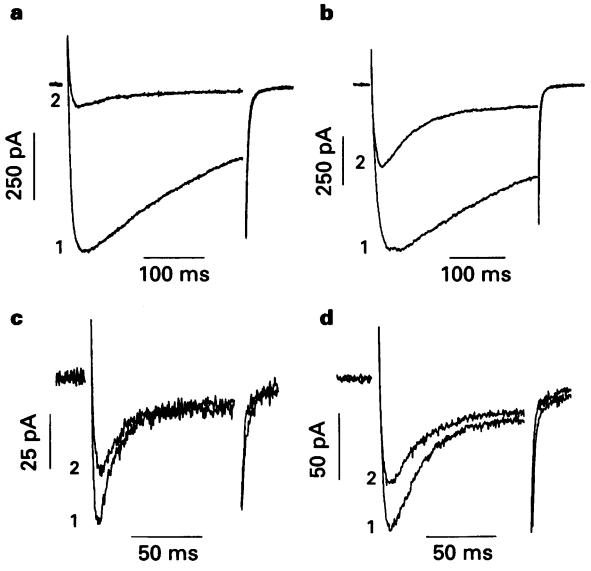

Figure 4 Stereoselectivity of isradipine action on $I_{Sr\text{-}HEK}$ and $I_{Sr\text{-}sH}$. HEK293 cells were depolarized every 10 s from a holding potential of -70 mV to a test potential of 0 mV (for observation of $I_{Sr\text{-}HEK}$) and to 20 mV (for observation of $I_{Sr\text{-}sH}$). Currents in the absence (1) and presence of drug (2), indicating I_{Sr}-inhibition in steady state, are superimposed. Experiments were performed on cells cultured in the presence of 10% FBS. (a) Inhibition of $I_{Sr\text{-}sH}$ (1-control) by 1 μM (+)-isradipine (2) and (b) block of $I_{Sr\text{-}sH}$ (1-control) by 1 μM (−)-isradipine (2). (c) Inhibition of $I_{Sr\text{-}HEK}$ (1) by 1 μM (+)-isradipine (2) and (d) $I_{Sr\text{-}HEK}$ (1) inhibition by 1 μM (−)-isradipine (2).

larization of the cell membrane from a holding potential of −50 mV to a test potential of 20 mV. The estimated values of the current density ranged from 1.0 up to 3.5 pA/pF (see also Table 1 for mean values).

$I_{Sr\text{-}sH}$ were sensitive to 1,4-dihydropyridines and increased more than 3 fold (mean of 3 experiments) at a test potential of 20 mV upon application of 1 μM)(±)-Bay K 8644, whereas application of (±)-Bay K 8644 (up to 10 μM) did not affect $I_{Sr\text{-}HEK}$. $I_{Sr\text{-}sH}$ were stereoselectively inhibited by the antagonist isradipine (Figure 4a, b). (+)-Isradipine (1 μM) blocked $I_{Sr\text{-}sH}$ by 87±2% ($n=3$) whereas the (−)-enantiomer was significantly less effective (with $P<0.01$) and induced only 61±3% ($n=3$) block.

Pharmacological features of $I_{Sr\text{-}HEK}$ were studied at a holding potential of −70 mV during depolarizing steps to 0 mV in HEK293 cells cultured in the presence of 10% FBS. Isradipine inhibited $I_{Sr\text{-}HEK}$ but the block was not stereoselective (Figure 4c, d). (+)-Isradipine (1 μM) induced a 30±4% ($n=3$) block whereas (−)-isradipine inhibited $I_{Sr\text{-}HEK}$ by 29±2% ($n=4$). A higher concentration (10 μM) of (+)- and (−)-isradipine blocked $I_{Sr\text{-}HEK}$ by 89±4% ($n=5$) and 88±8% ($n=3$) respectively. (−)-Nimodipine (10 μM) induced a similar amount of peak current inhibition (92±3% ($n=5$)). The block by isradipine was reversible (washout after 10 min 79±16% ($n=6$)), whereas block by (−) nimodipine was nearly irreversible (after 10 min washout less than 20% recovery). The 7-bromo substituted (±)-isradipine (VO 2605, 10 μM) that is almost inactive on L-type calcium channels (Glossmann & Ferry, 1985) also inhibited $I_{Sr\text{-}HEK}$ (block by 83±9%, $n=3$). Endogenous calcium channel currents were inhibited by Ni^{2+} with half maximal block occurring at 48±19 μM ($n=4$) (Figure 5a). The cone snail toxin ω-CTx MVIIC (1 μM) induced 20±3% ($n=4$) block of $I_{Sr\text{-}HEK}$ (Figure 5b) whereas ω-CTx GVIA (1 μM) induced 17±3% ($n=4$) current inhibition (Figure 5c). The funnel web spider toxin ω-Aga-IVA (200 nM) induced only weak inhibition (19±2%, $n=4$) of the endogenous calcium channel current (Figure 5d).

Discussion

The main purpose of the present study was to characterize the HEK293 cell line as an expression system for voltage-dependent calcium channels. We established that HEK293 cells, as previously shown for other expression systems, possess endogenous voltage-dependent calcium channel currents. The percentage of HEK293 cells expressing $I_{Sr\text{-}HEK}$ was even higher (76%) compared to CHO cells where only 24% of the cells were found to express endogenous calcium channels (Skryma *et al.*, 1994). The studied $I_{Sr\text{-}HEK}$ have a transient time course and are insensitive to the L-type calcium channel agonist (±)-Bay K 8644 (10 μM). Similar pharmacological features, including the weak inhibition of ω-Aga-IVA (Soong *et al.*, 1993, but see Ellinor *et al.*, 1993), ω-CTx GVIA (Soong *et al*,. 1993, but see Ellinor *et al.*, 1993) and ω-CTx MVIIC (Ellinor *et al.*, 1993) have been previously described for class E calcium channels (Williams *et al.*, 1994). In addition to its common pharmacological properties, the fast inactivation time course

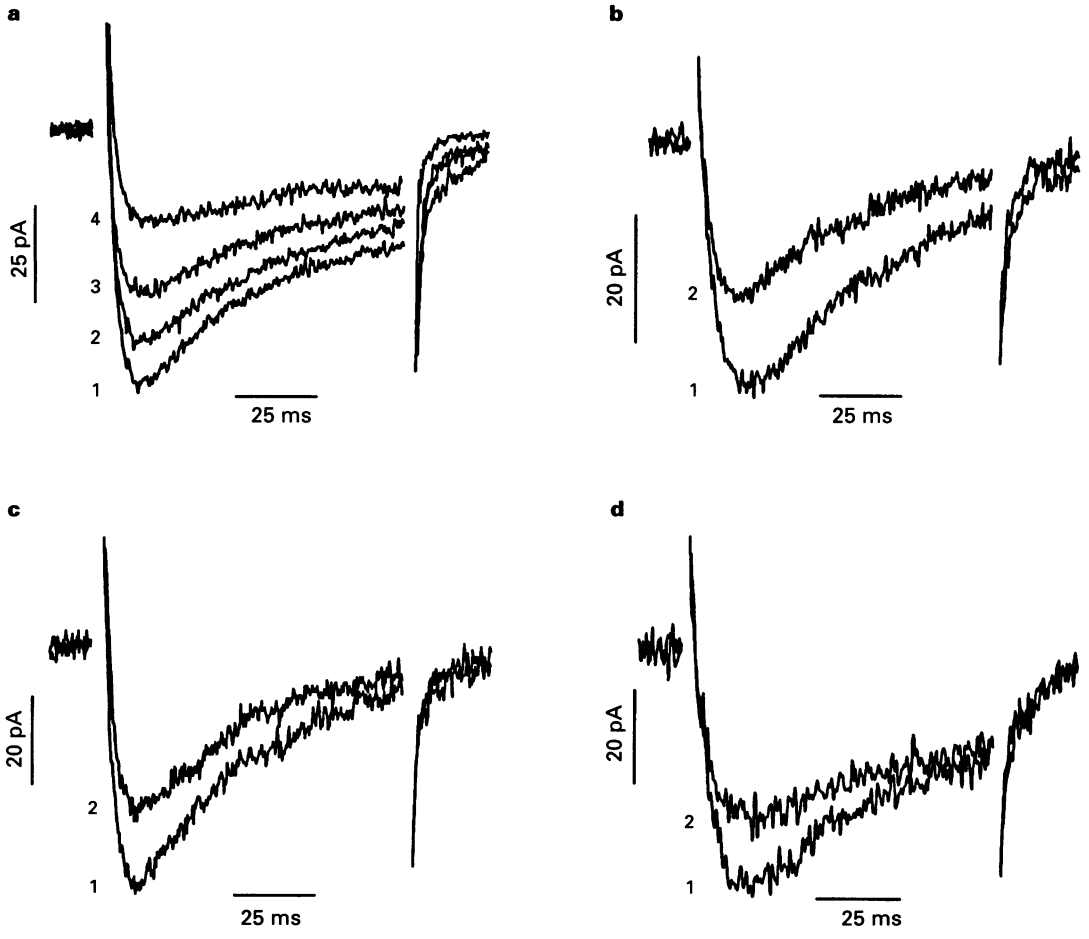

Figure 5 Pharmacological features of $I_{Sr\text{-}HEK}$. (a) Inhibition of $I_{Sr\text{-}HEK}$ (1) by subsequent application of 3 μM (2), 30 μM (3) and 100 μM (4) nickel. (b) Inhibition of $I_{Sr\text{-}HEK}$ (1) by 1 μM ω-CTx MVIIC (2); (c) Inhibition of $I_{Sr\text{-}HEK}$ (1) by 1 μM ω-CTx GVIA (2); (d) inhibition of $I_{Sr\text{-}HEK}$ (1) by 200 nM ω-Aga-IVA (2). $I_{Sr\text{-}HEK}$ were evoked by depolarizations from −70 mV to 0 mV applied at a frequency of 0.1 Hz.

of $I_{Sr\text{-}HEK}$ is also typical for class E calcium channels (Soong *et al.*, 1993; Ellinor *et al.*, 1993). Class E calcium channels inactivate with a time constant of about 70 ms (15 mM barium as charge carrier, Williams *et al.*, 1994) compared to $I_{Sr\text{-}HEK}$ inactivating with 10 mM strontium as charge carrier with a time constant of about 60 ms in the voltage range of −10 to 30 mV (see Figure 2a, b). The concentration for half maximal inhibition of $I_{Sr\text{-}HEK}$ (see Table 1) by Ni^{2+} ($IC_{50}=48$ μM) also corresponds to the reported half maximal inhibition of class E calcium channels (IC_{50} for current block by $Ni^{2+} \approx 30$ μM, Soong *et al.*, 1993; Ellinor *et al.*, 1993; Williams *et al.*, 1994).

Taken together, with respect to the established degree of identity in the pharmacology and kinetic properties, endogenous calcium channels in HEK293 cells share some properties with class E calcium channels (Soong *et al.*, 1993; Birnbaumer *et al.*, 1994).

In previous studies class E calcium channels have been reported to be insensitive to the 1,4-dihydropyridines, nifedipine (10 μM, Soong *et al.*, 1993) and nimodipine (10 μM, Ellinor *et al.*, 1993). The inhibition by isradipine and (−)-nimodipine distinguishes $I_{Sr\text{-}HEK}$ from class E channels. Inhibition of $I_{Sr\text{-}HEK}$ by isradipine was, however, not stereoselective and occurred at higher concentrations compared to the stereoselective block of $I_{Sr\text{-}sH}$ by the same drug (Figure 4). Additionally the 7-bromo-ester-substituted (±)-isradipine (VO2605) also inhibited $I_{Sr\text{-}HEK}$. This 7-bromo-ester-substitution (as in VO2605) is detrimental for L-type calcium channel binding (Glossmann & Ferry, 1985; Janis *et al.*, 1987). Thus, 1,4-dihydropyridine inhibition of $I_{Sr\text{-}HEK}$ clearly differs from that observed for L-type calcium channels.

Taken together, the endogenous calcium channel in HEK293 cells shares many characteristics with a low voltage-activated class E calcium channel or T-type channel described by Soong *et al.* (1993). However, this channel type does not fit precisely into any class of voltage-dependent calcium channels as defined by Birnbaumer *et al.* (1994), because of the following pharmacological properties: (i) non-stereoselective (but reversible) inhibition by isradipine and inhibition by (−)-nimodipine; (ii) no effect of (±)-Bay K 8644 and (iii) inhibition of $I_{Sr\text{-}HEK}$ by (±)-VO2605 with similar potency to that of isradipine. Clearly, this pharmacological profile for dihydropyridine compounds differs from that known for L-type calcium channels and further studies will show if endogenous calcium channels in HEK293 represent a new class of voltage-dependent calcium channels.

The important finding of this study is that whole cell calcium channel currents of expressed exogenous α_1 subunits in HEK293 cells can be contaminated by endogenous currents. The degree of contamination is dependent on the relation between the current densities of $I_{Sr\text{-}HEK}$ and the expressed L-type channel.

Schreieck *et al.* (1995) report L-type current densities in HEK293 cells (I_{Ba} measured with 30 mM barium as charge carrier) of more than 20 pA/pF if L-type α_1 subunits are expressed alone, and up to 200 pA/pF when other calcium channel subunits are co-expressed (compare with the current densities summarised in Table 1). However, as most studies were performed under different experimental conditions with respect to the chosen charge carrier (divalent cation), its concentration, and the time interval after transfection when currents were studied, it appears to be difficult to compare the observed current densities obtained in different laboratories.

Our data indicate, however, that it is possible to study functional properties of L-type α_1 calcium channel proteins in HEK293 cells: (i) First of all, the current density of L-type currents recorded 48 h after transfection ranged about one order of magnitude above the current density observed in non-transfected HEK293 cells which were cultured in a medium supplemented with 10% FBS. It has, nevertheless, to be emphasised that the density of endogenous calcium channels in HEK293 cells is dependent on the cell culture conditions and substantially increased if the cells are cultured in FBS-free culture medium (see Table 1). (ii) Because $I_{Sr\text{-}HEK}$ have a lower voltage for current activation, a possible contamination of expressed L-type calcium channels by $I_{Sr\text{-}HEK}$ can be substantially reduced if the membrane potential is held in the range −40 to −35 mV (see Figure 3) or corresponding prepulses are applied. Under these conditions more than 50% of the $I_{Sr\text{-}HEK}$ are in an inactivated non available state whereas L-type, calcium channel currents ($I_{Sr\text{-}sH}$) are completely available (Table 1, Figure 3). Furthermore, a contamination with $I_{Sr\text{-}HEK}$ can be observed at early stages after transfection if ramp depolarizations are applied (Figure 1d) and cells with a high density of $I_{Sr\text{-}HEK}$ can be excluded from analysis. (iii). Finally, the 'contamination' of whole cell L-type calcium channel currents by $I_{Sr\text{-}HEK}$ is dependent on the test pulse potential and will be small in the range of 10 to 30 mV because $I_{Sr\text{-}HEK}$ reach peak current values at more negative voltages (see Figure 1). Consequently, a contamination of L-type currents by endogenous calcium channel currents in HEK293 cells can be minimised if the experimental conditions (i.e. voltage protocols, cell culture conditions) are optimised and L-type calcium channels are expressed at high enough density.

We thank Prof. A. Schwartz for providing the $\alpha_{1C\text{-}a}$ cDNA, Dr D. Beech and Dr E.N. Timin for helpful suggestions and B. Kurka for expert technical assistance. This work was supported by grants from the FWF S 6601 (H.G.) and S 6603 (S.H.).

References

ADAMS, B.A. & BEAM, K.G. (1989). A novel calcium current in dysgenic skeletal muscle. *J. Gen. Physiol.*, **94.** 429–444.

BANGALORE, R., MEHRKE, G., GINGRICH, K., HOFMANN, F. & KASS, R.S. (1995). Gating currents of recombinant cardiac L-type calcium channels expressed in human embryonic kidney (HEK293) cells: relationships between charge movement and ionic current. *Biophys. J.*, **68,** A14.

BIEL, M., HULLIN, R., FREUNDNER, S., SINGER, D., DASCAL, N., FLOCKERZI, V. & HOFMANN, F. (1991). Tissue specific expression of high-voltage-activated dihydropyridin-sensitive L-type calcium channels. *Eur. J. Biochem.*, **200,** 81–88.

BIRNBAUMER, L., CAMPBELL, K.P., CATTERALL, W.P., HARPOLD, M.M., HOFMANN, F., HORNE, W.A., MORI, Y., SCHWARTZ, A., SNUTCH, T.P., TANABE, T. & TSIEN, R.W. (1994). The naming of voltage gated calcium channels. *Neuron*, **13,** 505–506.

BOURINET, E., FOURNIER, F., NARGEOT, J. & CHARNET, P. (1992). Endogenous *Xenopus*-oocyte Ca-channels are regulated by protein kinases A and C. *FEBS Lett.*, **299,** 5–9.

DE LEON, M., JOHNS, L., PEREZ-REYES, L., WEI, X., SOONG, T.W., SNUTCH, T.A & YUE, D.T. (1995). An essential structural domain for Ca-sensitive inactivation of L-type Ca channels. *Biophys. J.*, **68,** A13.

ELLINOR, P.T., ZHANG, J-F., RANDALL, A.D., ZHOU, M., SCHWARZ, T.L. & TSIEN, R.W. (1993). Functional expression of a rapidly inactivating neuronal calcium channel. *Nature*, **363,** 455–458.

GLOSSMANN, H. & FERRY, D.R. (1985). Assay for calcium channels. *Methods Enzymol.*, **109,** 513–589.

GRABNER, M., FRIEDRICH, K., KNAUS, H.-G., STRIESSNIG, J., SCHEFFAUER, F., STAUDINGER, R., KOCH, W.J., SCHWARTZ, A. & GLOSSMANN, H. (1991). Calcium channels from Cyprinus carpio skeletal muscle. *Proc. Natl. Acad. Sci. U.S.A.*, **88,** 727–731.

GRABNER, M., WANG, Z., HERING, S., STRIESSNIG, J. & GLOSSMANN, H. (1996). Transfer of 1,4-dihydropyridine sensitivity from L-type to class A (BI) calcium channels. *Neuron*, **16**, 207–218.

HAMILL, O.P., MARTY, A., NEHER, E., SAKMANN, B. & SIGWORTH, F.J. (1981). Improved patch-clamp techniques for high-resolution recording from cell and cell-free membrane patches. *Pflügers Arch.*, **391**, 85–100.

JANIS, R.A., SILVER, P.J. & TRIGGLE, D.J. (1987). Drug action and cellular calcium regulation. *Adv. Drug Res.*, **16**, 309–591.

KAMP, T.J., PEREZ-GARCIA, M.T. & MARBAN, E. (1995). Coexpression of β subunit with L-type calcium channel α_{1c} subunit in HEK293 cells increases ionic and gating currents. *Biophys. J.*, **68**, A349.

LACERDA, A.E., PEREZ-REYES, E., WEI, X., CASTELLANO, A. & BROWN, A.M. (1994). T-type and N-type calcium channels of *Xenopus* oocytes: evidence for specific interactions with β subunits. *Biophys. J.*, **68**, 1833–1843.

MIKAMI, A., IMOTO, K., TANABE, T., NIIDOME, T., MORI, Y., TAKESHIMA, H., NARUMIYA, S. & NUMA, S. (1989). Primary structure and functional expression of the cardiac dihydropyridine-sensitive calcium channel. *Nature*, **340**, 230–233.

PEREZ-GARCIA, M.T., KAMP, T.J. & MARBAN, E. (1995). Functional properties of cardiac L-type calcium channels transiently expressed in HEK293 cells. *J. Gen. Physiol.*, **105**, 289–306.

RUTH, P., RÖHRKASTEN, A., BIEL, M., BOSSE, E., REGULLA, S., MEYER, H.E., FLOCKERZI, V. & HOFMANN, F. (1989). Primary structure of the β-subunit of the DHP-sensitive calcium channel from skeletal muscle. *Science*, **245**, 1115–1118.

SAVCHENKO, A., GLOSSMANN, H. & HERING, S. (1995). Improved micro-perfusion chamber for multiple and rapid solution exchange in adherent single cells. *Pflügers Arch.*, **429**, 436–442.

SCHREIECK, J., ZONG, X.G., MEHRCE, G., FLOCKERZI, V., SCHMITT, C. & HOFFMANN, F. (1995). Transiently and stably expressed calcium channel subunit in HEK293 cells. *Naunyn-Schmied. Arch. Pharmacol.*, **351**, 376.

SKRYMA, R., PREVARSKAYA, N., VACHER, P. & DUFY, B. (1994). Voltage dependent Ca^{2+} channels in Chinese hamster ovary (CHO) cells. *FEBS Lett.*, **349**, 289–294.

SOONG, T.W., STEA, A., HODSON, C.D., DUBEL, S.J., VINCENT, S.R. & SNUTCH, T.P. (1993). Structure and functional expression of a member of low voltage-activated calcium channel family. *Science*, **260**, 1133–1135.

WANG, Z., GRABNER, M., BERJUKOW, S., SAVCHENKO, A., GLOSSMANN, H. & HERING, S. (1995). Chimeric L-type calcium channels expressed in *Xenopus laevis* oocytes reveal role of repeats III and IV in activation gating. *J. Physiol.*, **486**, 131–137.

WILLIAMS, M.E., MARUBIO, L.M., DEAL, C.R., HANS, M., BRUST, P.F., PHILIPSON, L.H., MILLER, R.J., JOHNSON, E.C., HARPOLD, M.M. & ELLIS, S.B. (1994). Structure and functional characterization of neuronal α_{1E} calcium channel subtypes. *J. Biol. Chem.*, **269**, 22347–22357.

(Received October 18, 1995
Revised January 17, 1996
Accepted February 9, 1996)